Original Paper

Neuro-Signals

Neurosignals 2012;20:252–264
DOI: 10.1159/000334960

Received: September 9, 2011
Accepted after revision: November 9, 2011
Published online: January 28, 2012

Temperature Dependence of Action Potential Parameters in *Aplysia* Neurons

Nam Gyu Hyun[a] Kwang-Ho Hyun[b] Kyungmin Lee[c] Bong-Kiun Kaang[d]

[a]Department of Physics, Jeju National University, Jeju, [b]Department of Biological Sciences, Korea Advanced Institute of Science and Technology, Kusung-Dong, [c]Department of Anatomy, Graduate School of Medicine, Brain Science & Engineering Institute, Kyungpook National University, Daegu, and [d]Department of Biological Science, National Creative Research Initiative Center for Memory, College of Natural Science, Seoul National University, Seoul, Korea

Key Words
Computational analysis · *Aplysia juliana* · Action potential parameters · Temperature dependence

Abstract
Although the effects of temperature changes on the activity of neurons have been studied in *Aplysia*, the reproducibility of the temperature dependence of the action potential (AP) parameters has not been verified. To this end, we performed experiments using *Aplysia* neurons. Fourteen AP parameters were analyzed using the long-term data series recorded during the experiments. Our analysis showed that nine of the AP parameters decreased as the temperature increased: the AP amplitude (A_{AP}), membrane potential at the positive peak (V_{pp}), interspike interval, first half (Δt_{r1}) and last half (Δt_{r2}) of the temperature rising phase, first half (Δt_{f1}) and last half (Δt_{f2}) of the temperature falling phase, AP ($\Delta t_{AP,\,1/2}$), and differentiated signal ($\Delta t_{DS,\,1/2}$) half-width durations. Five of the AP parameters increased with temperature: the differentiated signal amplitude (A_{DS}), absolute value of the membrane potential at negative peak ($|V_{np}|$), absolute value of the maximum slope of the AP during the temperature rising ($|-MSR|$) and falling ($|-MSF|$) phases, and spiking frequency (Frequency). This work could provide the basis for a better understanding of the elementary processes underlying the temperature-dependent neuronal activity in *Aplysia*.

Introduction

Temperature is one of the most important stimuli and produces numerous effects in most organisms. The effects of temperature change on the activities of neurons and axons have been studied in various species, including *Aplysia*, squids, snails, lobsters, crabs, crayfish, locusts, and frogs [1–8].

The large, well-studied neurons of *Aplysia* are suitable for studying the physiological effect of temperature because these neurons are long-lived in vitro compared to mammalian neural cells and so are apt to withstand heat stress for relatively long periods. Because of this, it is possible to obtain long-term intracellular recordings. The effects of heat stress on the neuronal activity of *Aplysia* have been observed as changes in the signal transduction pathways, synaptic physiology, muscle contractility, behavior, and neuronal firing patterns [9–13]. A regular and reproducible increase in the generation frequency of pacemaker potentials in *Aplysia* neurons between 5 and 25°C was found to be caused by an increase in temperature [14]. A temperature change from 10 to 20°C produced a noticeable hyperpolarization in the membrane of the right giant cell in the abdominal ganglion of *Aplysia californica* [15]. In other studies, the resistance increased with decreasing temperatures [1]; however, the burst duration (BD), spike height, and number of spikes per burst of the *Aplysia* R15

KARGER

Fax +41 61 306 12 34
E-Mail karger@karger.ch
www.karger.com

1424–862X/12/0204–0252$38.00/0

Accessible online at:
www.karger.com/nsg

Bong-Kiun Kaang
National Creative Research Initiative Center for Memory
Department of Biological Science, College of Natural Science
Seoul National University, San 56-1, Silim-dong, Kwanak-gu, Seoul 151-742 (Korea)
Tel. +82 2 880 7525, E-Mail kaang@snu.ac.kr

cell all decreased with an increase in temperature from 23 to 37°C [16]. Hakozaki et al. [17] examined the temperature-induced responses of the cells in an *Aplysia* ganglion, and their results suggested that a GTP-binding protein should be activated by raising the temperature to open the K^+ channels; however, few recent studies have reported any effect of temperature on the electrical activity of the *Aplysia* neurons.

Experiments involving action potential (AP) parameters using *Aplysia* neurons are found in papers published more than a decade ago, when there were few personal computer systems capable of calculating and saving large data files. This meant that it was difficult to determine the temperature dependence of AP parameters because of the slow acquisition rate when collecting data on a computer at the resolution shown on an oscilloscope. In the present study, we performed such an experiment using *Aplysia* neural cells in vitro over a long time and sought to determine the function describing the temperature dependence of the AP parameters with a high acquisition rate.

Although it is known that some AP parameters are altered with temperature for neurons within the *Aplysia* abdominal ganglion, it has not yet been verified whether the time dependence of these AP parameters is reproducible. Therefore, our aim was to determine which AP parameters for *Aplysia* neurons have reproducible temperature dependences. Because this experiment allowed recording over a relatively long period, we could include changes in temperature while monitoring individual neurons. We analyzed the recorded data using a computer program to obtain the quantitative temperature dependences of 14 AP parameters, which are defined in the next section.

Materials and Methods

Animals

The animals *(A. juliana)* were collected locally in Jeju, South Korea, and, prior to use, they were maintained in a recirculating sea water bath at 17°C. *A. juliana* has an appearance similar to that of *A. californica* in its body color patterns. However, the abdominal ganglion of *A. juliana* deviates in its overall structure from the prototypic ganglia of *A. californica* and *A. kurodai* [18].

Dissection

Before dissection, isotonic $MgCl_2$ amounting to half of each *A. juliana* specimen's weight was injected into it as an anesthetic. Abdominal ganglia were then removed from the specimens and incubated at 34°C for 35–65 min in 1% protease (type IX; Sigma) dissolved in a solution containing equal volumes of isotonic Leibovitz's L-15 medium (Cat. No. L-4386; Sigma) and artificial seawater (ASW; in mM: 460 NaCl, 10 KCl, 11 $CaCl_2$, 55 $MgCl_2$, and 10 HEPES; pH 7.6). They were then washed several times with ASW, and were rested in a low-temperature incubator (VS-1203PIN; Hanback Co., Daejeon, Korea) at 18°C for several hours. Finally, they were removed onto Petri dishes (50 × 9 mm), pinned down on Sylgard plates (Dow Corning, USA), and desheathed using fine scissors and tweezers.

Data Acquisition

Each abdominal ganglion was immersed in an L-15:ASW (1:1, v/v) medium, and the Petri dish with the abdominal ganglion was put on a small copper plate (50 × 100 mm), under which two thermoelectric coolers were set up side-by-side (HMN 3940; Acetec Co., Korea), one with the hot side facing up and one with the cold side facing up. The bath temperature was increased or decreased using a temperature controller system connected to the thermoelectric module. A PT100 platinum resistance temperature sensor was connected to a digital thermometer (TRM-006; Toho, Japan) to monitor the temperature. Intracellular recordings were obtained to measure the membrane potential. A line was connected to an electrode, which was inserted into a cell in the abdominal ganglion of *A. juliana* to obtain the values of the membrane potential, and was linked to channel 2. The PT100 temperature probe was placed near the abdominal ganglion. The membrane potential was measured using a Neuro Probe Amplifier (Model 1600; A-M Systems, Carlsborg, Wash., USA) with a microelectrode filled with 3 M KCl. Data were acquired using an A/D board (NI PCI-6221; National Instruments). The electrical signals of the APs were identified using a digital oscilloscope (54622A; Agilent, Colorado Springs, Colo., USA). Because we found that the beating or bursting cells generated APs at a rate of 0–4 Hz, it was necessary to record the data onto a computer hard disk at a rate of 3 kHz to clearly reproduce the APs. Thus, 180,000 pairs of temperature and AP values were automatically saved on the hard disk per minute, and each minute of data was stored under an independent file name over 60 h of recording, which amounted to approximately 20 GB of data. During this long, continuous recording period (~60 h), we inevitably encountered electrode slips and other problems. However, after reintroducing the electrode, we only continued the recording of cell data when the resting potential returned to its value (within ±2 mV) before the recording interruption. Otherwise, we stopped recording and did not include the data for further analysis.

Definitions of AP Parameters

The graph in figure 1A represents the AP, V(t). As shown in figure 1A, the positive peak membrane potentials $V_{pp,\,i-1}$ and $V_{pp,\,i}$ have approximately the same value of +30 mV at the two positive peak points $P_{pp,\,i-1}$ and $P_{PP,\,i}$ at the times $t_{pp,\,i-1}$ and $t_{pp,\,i}$, respectively. The negative peak membrane potentials $V_{np,\,i}$ and $V_{np\,i+1}$ have nearly the same value of –45 mV at the times $t_{np,\,i}$ and $t_{np,\,i+1}$ at the negative peak points $P_{np,\,i}$ and $P_{np,\,i+1}$, respectively. The graph in figure 1B represents the waveforms of the differentiated signals (DSs), which represent the digital differentiation of the membrane potential shown in figure 1A with respect to time. The digital differentiation has a maximum AP slope at the end of the temperature rising phase, MSR_i, at the positive peak point $Q_{DSpp,\,i}$ at the times $t_{DSpp,\,i}$. The digital differentiation also has an absolute maximum AP slope during the temperature falling

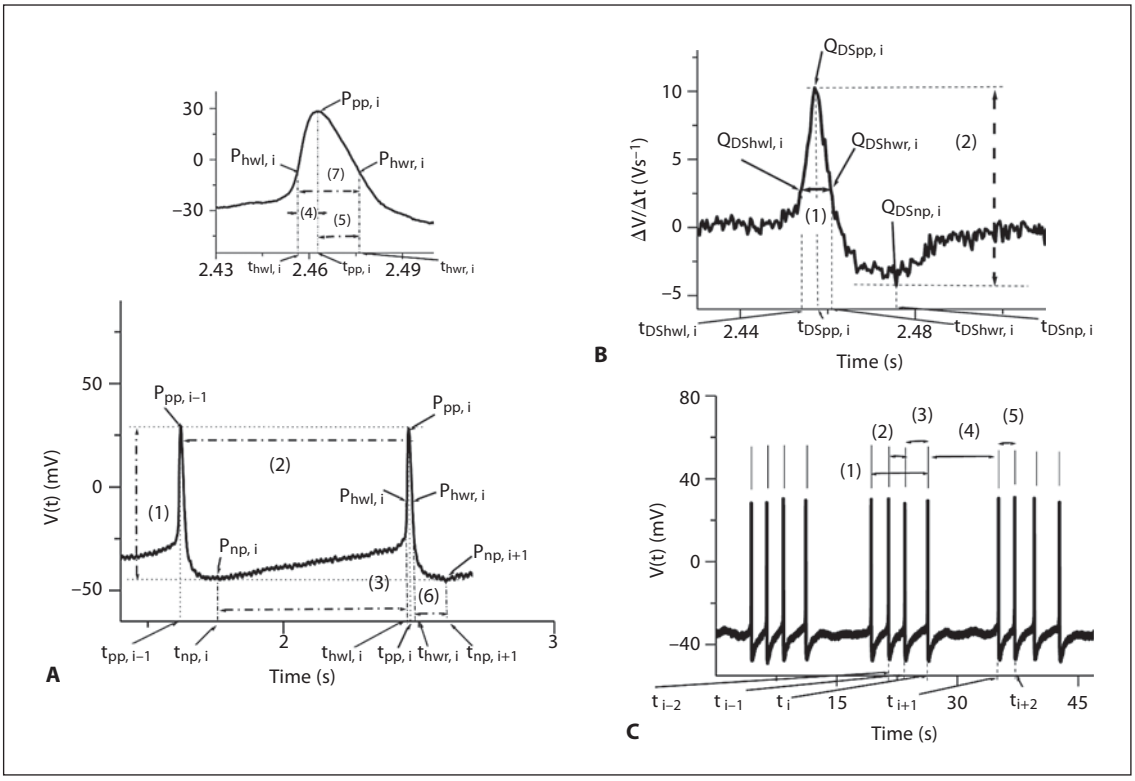

Fig. 1. Definitions of AP components. **A** The membrane potential vs. time for a neuron firing spontaneously. $P_{pp,\,i-1}$ and $P_{pp,\,i}$ designate arbitrary peak points and $t_{pp,\,i-1,}$ and $t_{pp,\,i}$ are the times corresponding to those points. A positive peak point occurs at the maximum point on the upper part of an AP. A negative peak point occurs at the minimum point on the lower part of an AP. The electrophysiological parameters measured include the potential difference [**A** (1): $A_{AP,\,i}$]; the duration between the two points $P_{pp,\,i-1}$ and $P_{pp,\,i}$ [**A** (2): ISI_i]; the time interval between the two points of a negative peak, $t_{np,\,i}$, and the half point of potential difference, $t_{hwl,\,i}$, during the rising phases of temperature change [**A** (3): $\Delta t_{r1,\,i}$]; the time interval between the half point of potential difference, $t_{hwl,\,i}$, and the point of a positive peak, $t_{pp,\,i}$ [**A** (4) in **inset:** $\Delta t_{r2,\,i}$]; the time duration between the two points of a positive peak, $t_{pp,\,i}$, and the half point of the potential difference, $t_{hwr,\,i}$, in the falling phase [**A** (5) in **inset:** $\Delta t_{f1,\,i}$]; the time duration between the half point of potential difference, $t_{hwr,\,i}$, and the point of the negative peak, $t_{np,\,i+1}$ [**A** (6): $\Delta t_{f2,\,i}$], and the time duration between the two points, $t_{hwl,\,i}$ and $t_{hwr,\,i}$, at the half amplitude membrane potential [**A** (7) in **inset:** $\Delta t_{AP,\,1/2,\,i}$]. The electrophysiological parameters calculated include the duration between the two points, $t_{DShwl,\,i}$ and $t_{DSwr,\,i}$ at the half amplitude DS [**B** (1): $\Delta t_{DS,\,1/2,\,i}$], maximum slope of action potentials during the rising phases of temperature change at the positive peak point, $Q_{DSpp,\,i}$ [**B**: MSR_i], minimum slope of AP during the falling phases of temperature change at the points of the negative peak, $Q_{DSnp,\,i}$ [**B**: MSF_i], and peak-to-peak amplitudes of DS [**B** (2): $A_{DS,\,i}$]. **C** The membrane potential vs. time for a neuron repeatedly firing discrete bursts of spikes [**C** (1): BD_i] followed by a quiescent period [**C** (4): IBI_i] before the next burst occurs. The electrophysiological parameters measured include the ISI in intraburst spikes [**C** (2): BI_i], the last ID of the spike train during a burst [**C** (3): $BI_{last,\,i}$], and the first ID of the spike train during a burst [**C** (5): $BI_{first,\,i}$].

phase, MSF_i, at the negative peak point $Q_{DSnp,\,i}$ at the times $t_{DSnp,\,i}$. The digital differentiation has half values for the maximum slopes of the APs at the two half-peak points $Q_{DShwl,\,i}$ and $Q_{DShwr,\,i}$ at the times $t_{DShwl,\,i}$ and $t_{DShwr,\,i}$, respectively. N is the number of spikes produced in 3 h, and the parameters of the somatic APs from giant and medium-sized neurons on the dorsal surface of the left caudal quarter-ganglion are defined as follows.

The AP amplitude, A_{AP} (mV), is defined as the mean peak-to-peak amplitude of the APs, where the term 'mean' indicates the average value of the parameter over 3 h [fig. 1A, (1)] ($A_{AP} \equiv \Sigma\, A_{AP,\,i}/N = \Sigma \mid V_{pp,\,i} - V_{np,\,i} \mid /N$). The membrane potential at the positive peak, V_{pp} (mV), is defined as the mean value of the membrane potentials at the points of positive peak, $V_{pp,\,i}$ (fig. 1A) ($V_{pp} \equiv \Sigma\, V_{pp,\,i}/N$). The membrane potential at the negative peak, V_{np} (mV), is defined as the mean value of the membrane potentials at the points of negative peak, $V_{np,\,i}$ (fig. 1A) ($V_{np} \equiv \Sigma\, V_{np,\,i}/N$). The interspike interval, ISI (ms), is defined as the mean interval duration (ID), ISI_i (or ID_i), of the neural spike trains, from $t_{pp,\,i-1}$ to $t_{pp,\,i}$ [fig. 1A, (2)] [$ISI \equiv \Sigma\, ISI_i/N$ (or $\Sigma\, ID_i/N$) $= \Sigma \mid t_{pp,\,i} - t_{pp,\,i-1} \mid /N$]. The first half of the temperature rising phase, Δt_{r1} (ms), is defined as the mean time interval, $\Delta t_{r1,\,i}$, between $t_{np,\,i}$ and $t_{hwl,\,i}$ [fig. 1A, (3)] ($\Delta t_{r1} \equiv \Sigma\, \Delta t_{r1,\,i}/N = \Sigma \mid t_{hwl,\,i} - t_{np,\,i} \mid /N$). The last half of the rising phase, Δt_{r2} (ms), is defined as the mean value of time interval, $\Delta t_{r2,\,i}$, between $t_{hwl,\,i}$ and $t_{pp,\,i}$ [fig. 1A, (4)]

($\Delta t_{r2} \equiv \Sigma\, \Delta t_{r2,\,i}/N = \Sigma \mid t_{pp,\,i} - t_{hwl,\,i} \mid /N$). The first half of the temperature falling phase, Δt_{f1} (ms), is defined as the mean value of time interval, $\Delta t_{f1,\,i}$, from $t_{pp,\,i}$ to $t_{hwr,\,i}$ [fig. 1A, (5)] ($\Delta t_{f1} \equiv \Sigma\, \Delta t_{f1,\,i}/N = \Sigma \mid t_{hwr,\,i} - t_{pp,\,i} \mid /N$). The last half of the falling phase, Δt_{f2} (ms), is defined as the mean value of time interval $\Delta t_{f2,\,i}$, between $t_{hwr,\,i}$ and $t_{np,\,i+1}$ [fig. 1A, (6)] ($\Delta t_{f2} \equiv \Sigma\, \Delta t_{f2,\,i}/N = \Sigma \mid t_{np,\,i+1} - t_{hwr,\,i} \mid /N$). The duration of the temperature rising phase, Δt_r (ms), is defined as the mean time interval from $t_{np,\,i}$ to $t_{pp,\,i}$ (fig. 1A) ($\Delta t_r = \Sigma \mid t_{pp,\,i} - t_{np,\,i} \mid /N \equiv \Delta t_{r1} + \Delta t_{r2}$). The duration of the temperature falling phase, Δt_f (ms), is defined as the mean value of time interval from $t_{pp,\,i}$ to $t_{np,\,i+1}$ (fig. 1A) ($\Delta t_f = \Sigma \mid t_{np,\,i+1} - t_{pp,\,i} \mid /N \equiv \Delta t_{f1} + \Delta t_{f2}$). The AP half-width duration, $\Delta t_{AP,\,1/2}$ (ms), is defined as the mean half-width duration, $\Delta t_{AP,\,1/2,\,i}$, between $t_{hwl,\,i}$ and $t_{hwr,\,i}$ [fig. 1A, (7)] ($\Delta t_{AP,\,1/2} \equiv \Sigma\, \Delta t_{AP,\,1/2,\,i}/N = \Sigma \mid t_{hwr,\,i} - t_{hwl,\,i} \mid /N$). The spontaneous firing frequency, simply referred to as Frequency (s^{-1}), is defined as the inverse of the ISI, i.e. Frequency $\equiv$ ISI^{-1}, where $ISI \equiv \Delta t_r + \Delta t_f = \Delta t_{r1} + \Delta t_{r2} + \Delta t_{f1} + \Delta t_{f2}$.

The maximum slope of the AP during the temperature rising phase, MSR (Vs^{-1}), is defined as the mean maximum value of digital differentiation, $\Delta V/\Delta t_{DSpp,\,i}$ (=MSR_i), at the points of the positive peaks, $Q_{DSpp,\,i}$ (fig. 1B) ($MSR \equiv \Sigma\, MSR_i/N$). The minimum slope of the AP during the temperature falling phase, MSF (Vs^{-1}), is defined as the mean minimum value of digital differentiation, $\Delta V/\Delta t_{DSnp,\,i}$ (=MSF_i), at the points of negative peaks, $Q_{DSnp,\,i}$ (fig. 1B) ($MSF \equiv \Sigma\, MSF_i/N$). The DS half-width duration, $\Delta t_{DS,\,1/2}$ (ms), is defined as the mean half-width duration, $\Delta t_{DS,\,1/2,\,i}$, from $t_{DShwl,\,i}$ to $t_{DShwr,\,i}$ [fig. 1B, (1)] ($\Delta t_{DS,\,1/2} \equiv \Sigma\, \Delta t_{DS,\,1/2,\,i}/N = \Sigma \mid t_{DShwr,\,i} - t_{DShwl,\,i} \mid /N$). The DS amplitude, A_{DS} (Vs^{-1}), is defined as the mean peak-to-peak amplitude of the DSs, $A_{DS,\,i}$ [fig. 1B, (2)] ($A_{DS} \equiv \Sigma\, A_{DS,\,i}/N = \Sigma \mid MSR_i - MSF_i \mid /N$). The burst duration (BD) (ms) is the mean duration of each burst, BD_i [fig. 1C, (1)] ($BD \equiv \Sigma\, BD_i/N$). Such bursts are followed by a quiescent period before the next burst occurs. The intraburst ISI, BI (ms), is defined as the mean ISI within bursts, BI_i, between t_{i-2} and t_{i-1} [fig. 1C, (2)] ($BI \equiv \Sigma\, BI_i/N = \Sigma \mid t_{i-1} - t_{i-2} \mid /N$). The last ID of the spike train during a burst, BI_{last} (ms), is defined as the mean last ID within bursts, $BI_{last,\,i}$, between t_{i-1} and t_i [fig. 1C, (3)] ($BI_{last} \equiv \Sigma\, BI_{last,\,i}/N = \Sigma \mid t_i - t_{i-1} \mid /N$). The first ID of the spike train during the burst, BI_{first} (ms), is defined as the mean first ID within bursts, $BI_{first,\,i}$, between t_{i+1} and t_{i+2} [fig. 1C, (5)] ($BI_{first} \equiv \Sigma\, BI_{first,\,i}/N = \Sigma \mid t_{i+2} - t_{i+1} \mid /N$). The interburst interval, IBI (ms), is defined as the mean time interval between two groups of spikes, IBI_i that are at least twice as far apart in time as $BI_{last,\,i}$ and $BI_{first,\,i}$ [fig. 1C, (4)] ($IBI \equiv IBI_i/N = \Sigma \mid t_{i+1} - t_i \mid /N$, on the condition that $IBI_i > 2 \cdot BI_{last,\,i}$ and $IBI_i > 2 \cdot BI_{first,\,i}$).

Computational Analysis of AP Components

The relationship between the current, I, flowing across the patch of membrane, the capacitive current, I_C, and the ionic current, I_i, is simple: I is the sum of I_C and I_i, i.e.

$$I = I_C + I_i, \tag{1}$$

where I is the stimulus current that initiated the action potential by depolarizing the cell above the threshold. When we performed experiments using *Aplysia* neurons, no external current was applied to generate APs. Therefore, the stimulus current was zero during the AP. Therefore,

$$I = I_C + I_i = C\frac{dV}{dt} + I_i = 0, \tag{2}$$

where C is the capacitance of the system. Thus, we find

$$I_i = -I_C = -C\frac{dV}{dt} \tag{3}$$

for nonpropagating APs [19]. The capacitance of a pair of plates of width A and length difference d, with a dielectric between the plates, is given by

$$C \equiv \frac{\varepsilon A}{d}, \tag{4}$$

where ε is the permittivity of the dielectric. If no biomembrane structural phase transition occurs in the cell membrane of a neuron in the *Aplysia* abdominal ganglion as its temperature changes from 8 to 34°C, the membrane capacitance of this cell will stay constant [20]. If C in equation (3) is constant, then $I_i \propto -dV/dt$, and thus $-C\,\Delta V/\Delta t$ can be qualitatively treated as equivalent to the ionic current. Thus, C (–MSR) and C (–MSF) can be interpreted as the maximum inward and maximum outward currents during the APs, respectively.

During the experiments, we obtained a vast amount of data. Every minute, 180,000 pairs of temperature and AP values were saved onto the hard disk. These data were consecutively and automatically recorded using an independent file name for each minute of data from 1 to 1,200. We kept recording new data for the next 1,200 min and so on. However, the mean values of each of the 14 AP parameters could be easily calculated using the computer program we designed.

If the value of temperature, T_j, and the value of membrane potential, V_j, were simultaneously recorded onto the computer hard disk at time t_j at a rate of 3,000 samples/s, then the minimum time interval was $\Delta t_j \equiv t_{j+1} - t_{j-1} = 2/3{,}000$ s. The first-order derivative of a digital function (in this case, voltage) by another variable (in this case, time) is defined using centered differences, as follows:

$$\begin{aligned}\frac{\Delta V}{\Delta t_j} &\equiv \frac{V_{j+1} - V_{j-1}}{t_{j+1} - t_{j-1}} \\ &= 3{,}000\,\frac{V_{j+1} - V_{j-1}}{2}\left(mVs^{-1}\right) \\ &= \frac{3}{2}\left(V_{j+1} - V_{j-1}\right)\left(Vs^{-1}\right).\end{aligned} \tag{5}$$

Electrophysiological data were processed using the scientific data analysis tools, C++, Origin 6.0, and Mathematica 5.1. All the data are presented as mean ± standard deviation in the text and table except in the figures where the data are presented as mean ± standard error.

Selection of Experimental Data for Further Analysis

To obtain reproducible temperature-dependent AP parameters, the transmembrane potentials and temperature values were obtained simultaneously from seven neurons. This resulted in about 300 experiments on neurons from the dorsal surface of the left caudal quarter-ganglion. Table 1 displays the conditions under which the seven experiments (A–G) were performed on separate animals. The weights of animals were between 115 and 324 g. The seasons during which the experiments were performed varied from winter to early summer. We chose cells with cell bodies larger than 100 μm in diameter. The media used were L-15 and ASW mixed in a ratio of 1:1 (volume to volume) or ASW only. The temperature

Table 1. Dissection conditions and electrophysiological properties of seven dissected *Aplysia* specimens

	Experimental data						
	exp. A	exp. B	exp. C	exp. D	exp. E	exp. F	exp. G
Weight of animal, g	235	251	252	115	275	152	324
Season of experiment	winter	summer	winter	spring	spring	spring.	spring
Media, ext. cell fluid	L-15:ASW (1:1, v/v)	ASW	L-15:ASW (1:1, v/v)	L-15:ASW (1:1, v/v)	L-15:ASW (1:1, v/v)	L-15:ASW (1:1, v/v)	L-15:ASW (1:1, v/v)
Temperature cycle range, °C	10.2–27.5	13.4-28.7	8.1–27.6	12.4–33.7	12.6–26.0	14.1–33.9	12.2–27.8
Total recording time, min	3,943	720	3,496	1,174	1,800	2,165	906
Total number of spikes	360,845	88,858	298,030	108,954	64,756	60,357	84,431
Average firing rate, min^{-1}	91.5	123.4	85.2	92.8	35.9	27.8	93.1
sel. dur. for anal., min (n of rep. tem. changes)	1,800 (16)	580 (4)	854 (8)	792 (7)	1,163 (8)	801 (7)	727 (5)
Spon. firing patterns	beating	beating	beating	beating	beating	bursting	bursting

These are shown as 7 separate experiments, named A–G. ext. cell fluid = External cell fluid; sel. dur. for anal. = selected section duration for analysis; n of rep. tem. changes = number of repetitive temperature changes; Spon. firing patterns = spontaneous firing patterns; v/v = volume/volume.

was varied between 8.1 and 33.9°C and 4–16 temperature cycles were used. The total length of time over which the transmembrane potentials were recorded varied between 720 and 3,943 min. The total numbers of spikes in the transmembrane potential varied from 60,537 to 360,845. The average firing rates for the experiments were between 35.9 and 123.4 min^{-1}. Both beating and bursting spontaneous firing patterns were observed in the acquired data.

Results

We calculated the maximum and minimum values for 10 of the AP parameters and the IBI using the experimental data shown in table 1 and analyzed the temperature dependence of these parameters. We found qualitative changes in these parameters as the temperature increased. These values and their temperature dependences are summarized in table 2. The ranges of the A_{AP}, V_{pp}, $\Delta t_{AP,\,1/2}$, Δt_{r1}, Δt_{r2}, Δt_{f1}, Δt_{f2}, Frequency, $|-MSR|$, $|-MSF|$, and IBI values are 47.3–89.5 mV, 0.3–44.7 mV, 2.9–21.1 ms, 235–4,170 ms, 1.2–6.9 ms, 1.7–15.4 ms, 13.2–136.7 ms, 0.2–3.3 s^{-1}, 9.2–32.2 Vs^{-1}, 4.1–20.4 Vs^{-1}, and 4.5–22.3 s, respectively. The values of A_{AP}, V_{pp}, $\Delta t_{AP,\,1/2}$, Δt_{r2}, Δt_{f1}, Δt_{r1}, Δt_{f2}, and IBI decreased as the temperature increased; in some cells, Δt_{r1} and Δt_{f2} increased slightly after the minimum value was reached. However, the values of $|-MSF|$, $|-MSR|$, and Frequency increased with temperature; in some cells, they decreased after the maximum value was reached.

In order to obtain a more quantitative analysis of the temperature dependences of the AP parameters from the acquired data shown in tables 1 and 2, we focused on the two data sets recorded from two spontaneously beating neurons (experiments A and C). We found that the standard errors of the means of the AP parameters were much smaller in these two cells than in the other cells (experiments B and D–G), which allowed a quantitative analysis.

A comparison of the temperature dependences of the data (experiments A and C) is shown in figure 2. The characteristics of the temperature dependences of the 14 AP parameters of the two experiments are similar. Nine parameters, A_{AP}, V_{pp}, $\Delta t_{AP,\,1/2}$, $\Delta t_{DS,\,1/2}$, ISI, Δt_{r1}, Δt_{r2}, Δt_{f1}, and Δt_{f2}, decreased, whereas the other 5 parameters, $|V_{np}|$, A_{DS}, $|-MSR|$, $|-MSF|$, and Frequency, increased as the temperature increased. Furthermore, two cells showed similar quantitative changes in most of the AP parameters in response to a temperature change. However, the values of V_{np} were different in the cells because V_{np} is related to the resting membrane potential (V_r), which is known to differ greatly depending on the cell type. Taken together, these qualitative and quantitative analyses suggest that the temperature-dependent changes in most of the AP parameters could be general phenomena in *Aplysia* neurons.

Although the mean values of the AP parameters and the experimental conditions for experiments A and C were similar, we further analyzed the data from experi-

Table 2. Analysis results for ten AP parameters and IBI: maximum values, minimum values, and analyzed patterns of temperature dependence

AP parameters	External values and patterns	External values and patterns of APs						
		exp. A	exp. B	exp. C	exp. D	exp. E	exp. F	exp. G
A_{AP}, mV	max. values	78.0 ± 1.9	84.7 ± 3.9	70.3 ± 1.3	79.9 ± 3.9	81.0 ± 5.7	89.5 ± 8.3	78.4 ± 1.2
	min. values	55.3 ± 2.4	61.8 ± 6.6	59.7 ± 1.0	47.3 ± 3.6	49.0 ± 4.2	77.8 ± 3.4	57.3 ± 1.3
	patterns of tem. dep.	↓	↓	↓	↓	↓	↓	↓
V_{pp}, mV	max. values	32.3 ± 2.6	41.3 ± 2.1	34.0 ± 1.1	44.7 ± 1.5	41.3 ± 6.7	21.2 ± 7.4	26.5 ± 1.1
	min. values	1.0 ± 2.9	19.8 ± 3.9	19.2 ± 1.0	16.2 ± 1.8	8.4 ± 6.7	6.4 ± 3.3	0.3 ± 1.1
	patterns of tem. dep.	↓	↓	↓	↓	↓	↓	↓
$\Delta t_{AP, 1/2}$, ms	max. values	17.8 ± 1.6	8.4 ± 0.9	20.2 ± 1.3	15.3 ± 4.1	9.2 ± 1.4	21.1 ± 1.6	7.9 ± 0.4
	min. values	5.3 ± 0.4	3.7 ± 0.4	5.5 ± 0.1	5.5 ± 1.4	2.9 ± 0.9	4.7 ± 0.4	4.0 ± 0.3
	patterns of tem. dep.	↓	↓	↓	↓	↓	↓	↓
Δt_{r1}, ms	max. values	1,680 ± 462	616 ± 112	1,836 ± 139	1,360 ± 735	4,170 ± 2,507	1,304 ± 1,096	1,318 ± 288
	min. values	321 ± 51	235 ± 47	250 ± 5	419 ± 58	706 ± 125	670 ± 160	329 ± 42
	patterns of tem. dep.	↓	↓	↓	↓	↓↑	↓↑	↓
Δt_{r2}, ms	max. values	6.1 ± 0.3	2.8 ± 0.3	6.9 ± 0.4	4.9 ± 1.0	3.3 ± 0.4	5.7 ± 1.6	2.8 ± 0.1
	min. values	2.2 ± 0.2	1.5 ± 0.3	2.5 ± 0.0	2.0 ± 0.4	1.2 ± 0.5	2.0 ± 0.3	1.8 ± 0.1
	patterns of tem. dep.	↓	↓	↓	↓	↓	↓	↓
Δt_{f1}, ms	max. values	11.6 ± 1.3	5.6 ± 0.6	13.2 ± 0.9	10.4 ± 3.1	5.8 ± 1.0	15.4 ± 1.5	5.0 ± 0.3
	min. values	3.1 ± 0.1	2.2 ± 0.3	3.0 ± 0.1	3.4 ± 1.1	1.7 ± 0.6	2.6 ± 0.2	2.1 ± 0.3
	patterns of tem. dep.	↓	↓	↓	↓	↓	↓	↓
Δt_{f2}, ms	max. values	118.4 ± 8.0	136.7 ± 17	107.8 ± 13	97.0 ± 16	87.2 ± 37.2	49.5 ± 11.7	134.8 ± 302
	min. values	35.8 ± 11.0	59.1 ± 9.3	39.0 ± 2.2	37.1 ± 2.6	37.2 ± 4.0	13.2 ± 1.0	34.9 ± 3.4
	patterns of tem. dep.	↓	↓↑	↓	↓↑	↓↑	↓	↓
Frequency, s^{-1}	max. values	2.9 ± 0.5	2.7 ± 0.4	3.3 ± 0.0	2.1 ± 0.2	1.3 ± 0.2	1.5 ± 0.3	2.7 ± 0.3
	min. values	0.5 ± 0.1	1.4 ± 0.2	0.5 ± 0.0	0.8 ± 0.3	0.2 ± 0.0	1.0 ± 0.4	0.7 ± 0.1
	patterns of tem. dep.	↑	↑	↑	↑	↑↓	↑↓	↑
|–MSR|, Vs^{-1}	max. values	20.0 ± 1.8	32.2 ± 5.2	16.0 ± 0.3	23.5 ± 1.5	26.9 ± 2.4	27.5 ± 0.6	25.7 ± 1.3
	min. values	11.0 ± 0.7	25.2 ± 4.2	9.2 ± 0.1	14.0 ± 2.3	19.5 ± 3.0	17.6 ± 3.4	20.6 ± 1.2
	patterns of tem. dep.	↑	↑↓	↑↓	↑↓	↑↓	↑	↑↓
|–MSF|, Vs^{-1}	max. values	10.9 ± 0.3	20.4 ± 7.2	9.0 ± 0.4	11.5 ± 1.9	17.3 ± 2.0	16.7 ± 5.0	11.3 ± 1.4
	min. values	4.5 ± 0.4	8.3 ± 3.5	4.1 ± 0.6	4.6 ± 1.5	8.8 ± 1.5	5.2 ± 0.4	6.3 ± 0.5
	patterns of tem. dep.	↑	↑	↑	↑↓	↑	↑	↑
IBI, s	max. values						22.3 ± 9.9	21.6 ± 4.1
	min. values						4.5 ± 1.0	7.4 ± 1.6
	patterns of tem. dep.						↓	↓

These patterns show the overall qualitative changes as temperature increased: ↓ = decrease; ↑ = increase; ↓↑ = first decrease, then increase; ↑↓ = first increase, then decrease.

max. = Maximum ; min. = minimum ; patterns of tem. dep. = patterns of temperature dependence.

ment A for the following reasons. The total recording time was longer and the total number of spikes in experiment A was greater than those in experiment C. During experiment C, we repeatedly saw bursting activities in the low temperature regions; however, during experiment A, there was a regular beating activity for a duration of 1,200 min without any typical bursting activity. Thus, experiment A showed the longest recording time, longest selected duration, and a regular beating activity. For these reasons, the data from experiment A were chosen for further analysis. However, not all of the data from experiment A were useful for analysis. Thus, we had to select a good section from the data recorded during experiment A to determine functional relations that describe the temperature dependences of the AP parameters. To this end, it was necessary to examine the experimental condi-

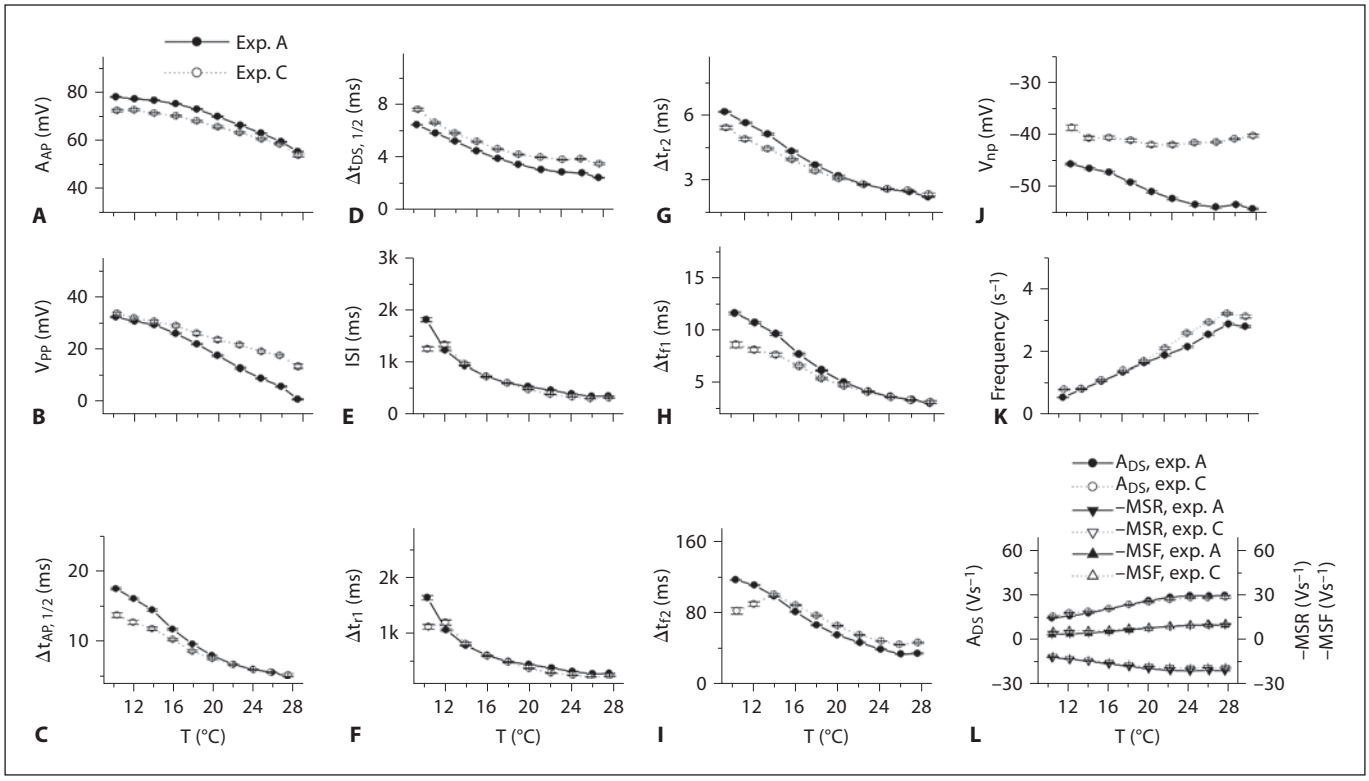

Fig. 2. Comparison of temperature dependences of 14 AP parameters between experiments A and C. The data in the 'selected duration for analysis' section in table 1 were averaged. The overall tendencies listed in table 2 are clearly shown in these figures.

tions in detail by plotting A_{AP} and temperature, T, as a function of time, as described below.

The upper trace in figure 3 is A_{AP}, and the lower trace is the temperature. The temperature was maintained at room temperature for the first 400 min. The temperature value and some AP parameters were calculated between 81 and 320 min. This is represented by (a) in the upper left corner in figure 3 ($T = 18.70 \pm 0.15$°C, $\Delta t_{AP,\,1/2} = 8.58 \pm 0.38$ ms, Frequency = 2.01 ± 0.12 s^{-1}, IBI = 0, and $A_{AP} = 75.01 \pm 0.79$ mV). Because of the low standard errors, the spiking pattern could be considered as regular while the temperature was held constant. Over the period from 401 to 3,943 min, we varied the temperature between 9 and 28°C. Over this time, the mean temperature was 20.12 ± 5.77°C. Both heating and cooling occurred at an average rate of approximately 0.3°C min^{-1}. No AP data were recorded between 394 and 442 min because the electrode slipped from the cell during the experiment for some unknown reason. It can also be seen from the upper trace of figure 3 that the value of A_{AP} was unstable between 360 and 560 min. However, because the cell kept spiking in a regular and reasonable manner after 560 min, it was thought that this did not greatly affect the data to be analyzed. It was useful to analyze the data represented by (b), in the upper middle part of this graph and recorded between 601 and 2,400 min, under a periodically alternating temperature; the mean A_{AP} value over this period was 67.80 ± 8.25 mV. The data after 2,400 min were not useful for analysis because the values of A_{AP} dropped and silent types of firing patterns appeared after 3,000 min. Finally, it was necessary to determine whether the spiking pattern of this selected section was influenced by bursting activity.

Bursting is one of the three signaling patterns of neurons, and in bursting patterns, silent periods are followed by periods of spiking. All of the bursting activities could be calculated from the 30 consecutive hours of data that were saved between 601 and 2,400 min. Spontaneous bursting activities did not occur for the time period from 601 to 1,837 min; however, seven bursting patterns were found between 1,838 and 1,842 min, and these occurred at a temperature of approximately 10°C (BI = 2.57 ±

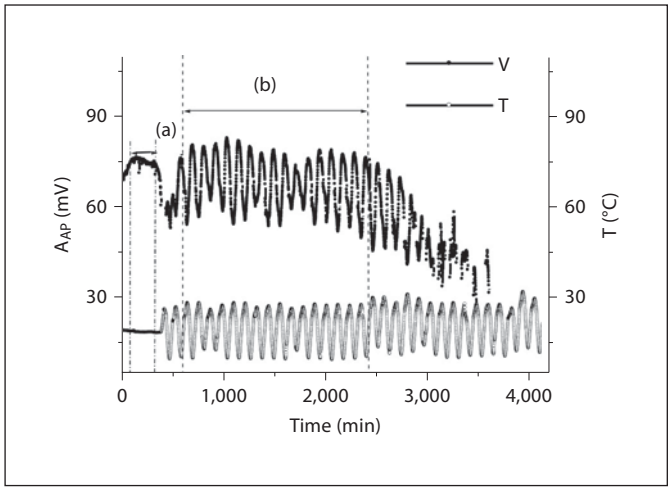

Fig. 3. Changes in A_{AP} and temperature with time. A_{AP} (upper trace) is represented by the symbol (a) under a constant temperature and by the symbol (b) selected for analysis under the periodically alternating temperature. The temperature (T) (lower trace) was changed periodically between 10.2 and 27.5°C. V = Membrane potential.

0.148 s and IBI = 6.53 ± 0.819 s). They occurred 54 more times with their durations totaling 19 min between 1,843 and 2,320 min. Because the ratios of IBI to BI (IBI/BI) of these bursting activities at low temperatures were between 2.3 and 3.2, the spiking patterns of these bursting activities were not fundamentally different from beating activities. A typical bursting activity, in which the IBI to BI ratio became 19.5, occurred only once, at 2,321 min, at a temperature of 20.7°C. From this, we can conclude that the spiking analysis of the selected section was not influenced by the effects of bursting activity. Finally, we selected a good section of data from experiment A, specifically the data recorded between 601 and 2,400 min, to discuss the temperature dependences of the AP parameters. Before presenting these results, it is necessary to give a brief account of the statistical method used to treat the experimental data.

Figures could be plotted using the experimental data recorded between 601 and 2,400 min presented by (b) in figure 3. In this section, there were a total of 211,698 spikes; therefore, each of the 1,800 files contains an average of 117.6 APs. First, the mean values of the AP parameters at each corresponding temperature were calculated, one file at a time, using a C++ program, and the results were saved to text files. The saved files were then copied to the Origin program and sorted by temperature. The files were divided into ten groups, each corresponding to a 2°C temperature interval, and each group contained 180 values for each of the AP parameters. In the Origin program, the averages of the 180 values for each AP parameter were calculated; each filled dot in figure 2 is an average of 21,169 measurements of APs, averaged with error bars. Each data point in figures 4–6 is an average of 10,585 measurements; the temperature rising and falling phases and the first and second half-time periods are plotted separately in the numbered panels of the same subfigure, i.e. in figures 4A1–6C1 and figures 4A2–6C2, respectively. It is possible to draw multiple plots in figure 4 using these mean values for the AP parameters, and it is not difficult to find apparently reproducible temperature dependences for the AP parameters in these figures.

AP Parameters That Decreased with Increasing Temperature

As shown in figures 4A–C, the parameters A_{AP}, V_{pp}, $\Delta t_{AP,\,1/2}$, and $\Delta t_{DS,\,1/2}$ all decreased as the temperature was raised. The standard errors of these values were small. The values of A_{AP} and V_{pp} during the falling phases were almost identical to those during the rising phases of temperature change (fig. 4A1). The values of A_{AP} and V_{pp} from 1 to 900 min were also very similar to those from 901 to 1,800 min (fig. 4A2). Figure 4B1 presents plots of $\Delta t_{AP,\,1/2}$ as a function of temperature. The values of $\Delta t_{AP,\,1/2}$ were very similar, irrespective of the rising or falling phases of the temperature changes. The values of $\Delta t_{AP,\,1/2}$ from 1 to 900 min were a little larger than those from 901 to 1,800 min, and the difference between the two sets of values increased as the temperature was decreased (fig. 4B2). The DS half-width duration, $\Delta t_{DS,\,1/2}$, was calculated as the width at half-maximum amplitude of A_{DS}. Figure 4C presents plots of $\Delta t_{DS,\,1/2}$ as a function of temperature. The values of $\Delta t_{DS,\,1/2}$ during the rising phases were slightly larger than those during the falling phases of temperature change at low temperatures, whereas at high temperatures, the values of $\Delta t_{DS,\,1/2}$ during the falling phases were slightly larger than those during the rising phases of temperature change (fig. 4C1). The values of $\Delta t_{DS,\,1/2}$ from 1 to 900 min were slightly higher than those from 901 to 1,800 min, but it was reversed at low temperatures (fig. 4C2).

Plots of ISI, Δt_{r1} and Δt_{r2}, and Δt_{f1} and Δt_{f2} as functions of temperature are shown in figure 5A–C, respectively. The values of ISI and Δt_{r1} during the rising phases were slightly larger than those during the falling phases of temperature change (fig. 5A1). The values of ISI and Δt_{r1} from 901 to 1,800 min were slightly larger than those from 1 to 900 min, and the difference between these two

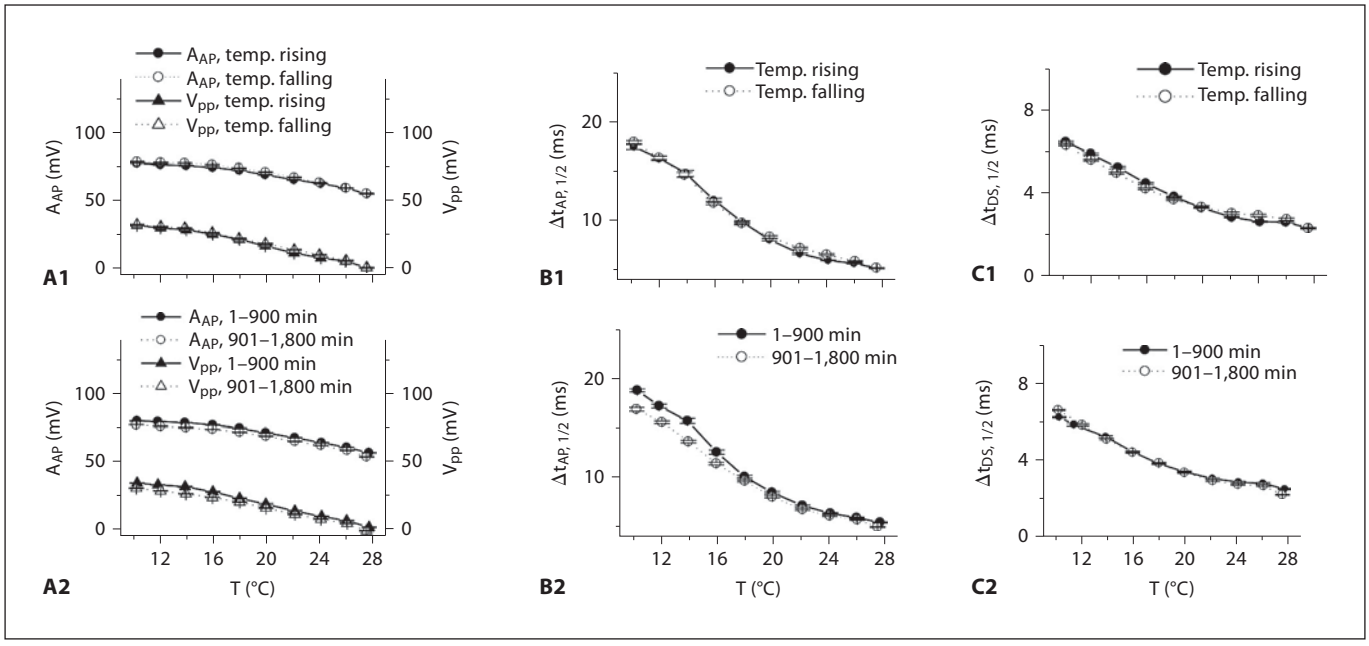

Fig. 4. Decreases in AP parameters with temperature increase. A_{AP}, $\Delta t_{AP,\,1/2}$, $\Delta t_{DS,\,1/2}$ and V_{pp} (during the rising and falling phases of temperature change) as a function of temperature are shown in **A1**, **B1**, **C1**, and **A1**, respectively. A_{AP}, $\Delta t_{AP,\,1/2}$, $\Delta t_{DS,\,1/2}$ and V_{pp} (from 1 to 900 min and from 901 to 1,800 min) as a function of temperature are shown in **A2**, **B2**, **C2**, and **A2**, respectively.

values increased slightly at lower temperatures (fig. 5A2). The values of Δt_{r2} during the rising phases were slightly larger than those during the falling phases of temperature change at low temperatures; however, at high temperatures, the values of Δt_{r2} during the falling phases were slightly larger than those during the rising phases of temperature change. In contrast, the values of Δt_{f1} during the temperature falling phases were slightly larger than those during the temperature rising phases (fig. 5B1). The values of Δt_{r2} and Δt_{f1} from 1 to 900 min were slightly larger than those from 901 to 1,800 min; however, in the latter case, the difference between the two values became larger as the temperature decreased (fig. 5B2). Figure 5C presents plots of Δt_{f2} as a function of temperature. The values of Δt_{f2} during the rising phases were slightly larger than those during the falling phases of temperature change (fig. 5C1). In addition, the values of Δt_{f2} from 901 to 1,800 min were slightly larger than those from 1 to 900 min between 18 and 28°C, and the difference between these two values increased with temperature (fig. 5C2).

AP Parameters That Increased with Temperature

Plots of V_{np}, A_{DS}, –MSR and –MSF, and Frequency as functions of temperature are shown in figure 6, respectively. The absolute values of V_{np} during the temperature falling phases were slightly larger than those during the temperature rising phases at low temperatures, but it was reversed at high temperatures (fig. 6A1). The absolute values of V_{np} from 901 to 1,800 min were slightly larger than those from 1 to 900 min at low temperatures, but not at high temperatures (fig. 6A2). The parameters A_{DS}, –MSF, and –MSR are plotted in figure 6B as functions of temperature. The DS amplitude, A_{DS}, was defined as the absolute value of the difference between –MSR and –MSF, i.e. $A_{DS} \equiv |\,(\text{–MSF}) - (\text{–MSR})\,|$. The parameters A_{DS}, |–MSF|, and |–MSR| all increased with temperature. The values of A_{DS}, |–MSF|, and |–MSR| during the temperature falling phases were almost identical to those during the temperature rising phases (fig. 6B1). The values of A_{DS}, |–MSF|, and |–MSR| from 1 to 900 min were also almost identical to those from 901 to 1,800 min (fig. 6B2).

The spike frequency (Frequency) is plotted in figure 6C as a function of temperature. The Frequency values during the temperature falling phases were slightly larger than those during the temperature rising phases between 10 and 26°C. The difference between the Frequency values of the rising and falling phases increased as the temperature increased. However, at 28°C, the Frequency val-

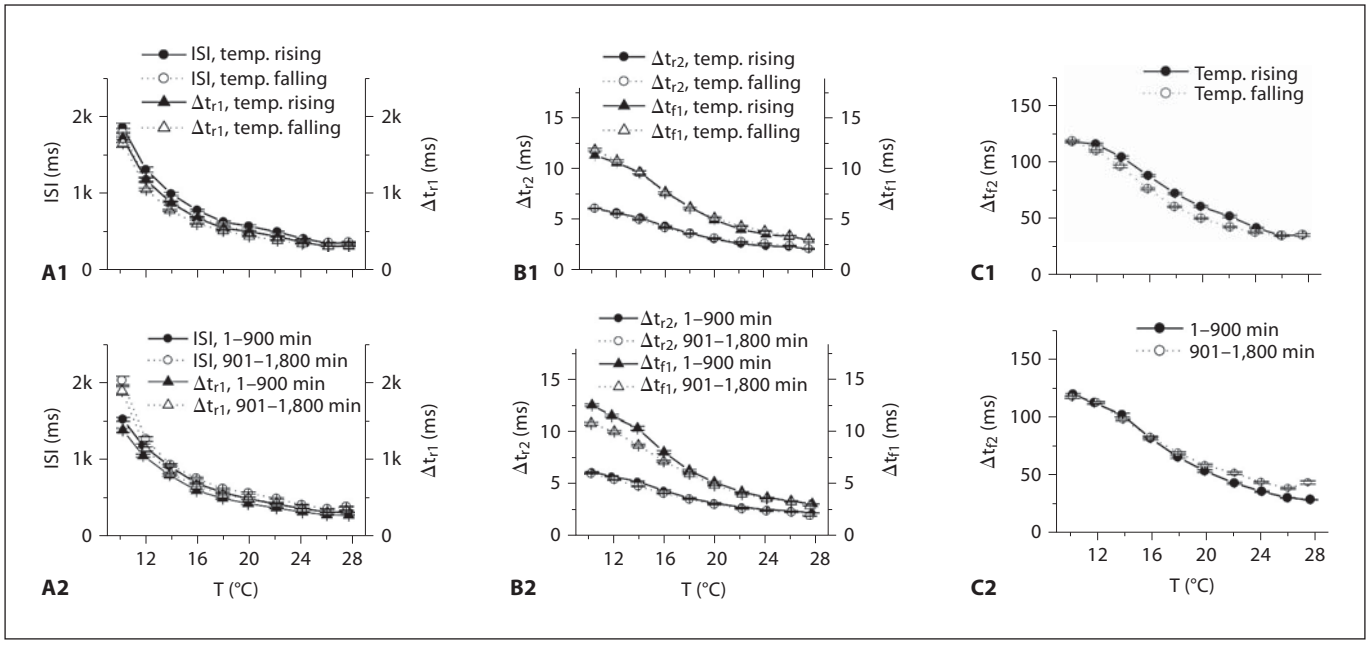

Fig. 5. Decreases in AP parameters with temperature increase. ISI, Δt_{r2}, Δt_{f2}, Δt_{r1}, and Δt_{f1} (during the rising and falling phases of temperature change) as a function of temperature are shown in **A1**, **B1**, **C1**, **A1**, and **B1**, respectively. ISI, Δt_{r2}, Δt_{f2}, Δt_{r1}, and Δt_{f1} (from 1 to 900 min and from 901 to 1,800 min) as a function of temperature are shown in **A2**, **B2**, **C2**, **A2**, and **B2**, respectively.

ues during the temperature rising phases were slightly larger than those during the temperature falling phases (fig. 6C1). The Frequency values from 1 to 900 min were slightly larger than those from 901 to 1,800 min (fig. 6C2).

Discussion

All animals that are active over a range of temperatures require an internal temperature system constructed of individual temperature-sensitive reactions in order to maintain function throughout the entire temperature range. For example, circadian oscillators cannot allow the period of their clock to change in response to a change in temperature [11]. In this study, we showed that 14 AP parameters changed in response to a temperature change in *Aplysia* neurons. However, the functional implications or evolutionary explanations of these temperature-dependent changes in the AP parameters are still unclear. They may be involved in the process of temperature detection by changing the AP frequency and/or other parameters, or they could be part of the cell's protective response to temperature shocks. One aim of this study was to understand the underlying mechanism of the electrophysiological response of a neuron to temperature change in terms of ionic currents by using *Aplysia* neurons as an experimental model. We would like to eventually define this temperature-driven response of a neuron using a set of mathematical equations composed of ionic currents. In order to accomplish this, we need to acquire quantitative data such as the 14 AP parameters analyzed in this study.

Experiments involving temperature-dependent AP parameters such as A_{AP}, $\Delta t_{AP,\,1/2}$, frequency, and resting membrane potential (V_r) in *Aplysia* neurons have previously been performed [13, 14, 16]. The general conclusion from these past studies on *Aplysia* neuronal firing patterns is that a rising temperature increases the spike frequency [14, 21] and absolute value of the resting membrane potential [13, 14], and that there is a correlation with a decrease in the spike amplitude and $\Delta t_{AP,\,1/2}$ [16]. However, the analysis methods used in the past had limitations from a technical point of view because they dealt with the temperature dependences of AP parameters by depending on the data acquired from a pen writer or magnetic tapes over a relatively short time interval. It was possible for us to use a higher resolution in the functional relations that described the temperature dependences

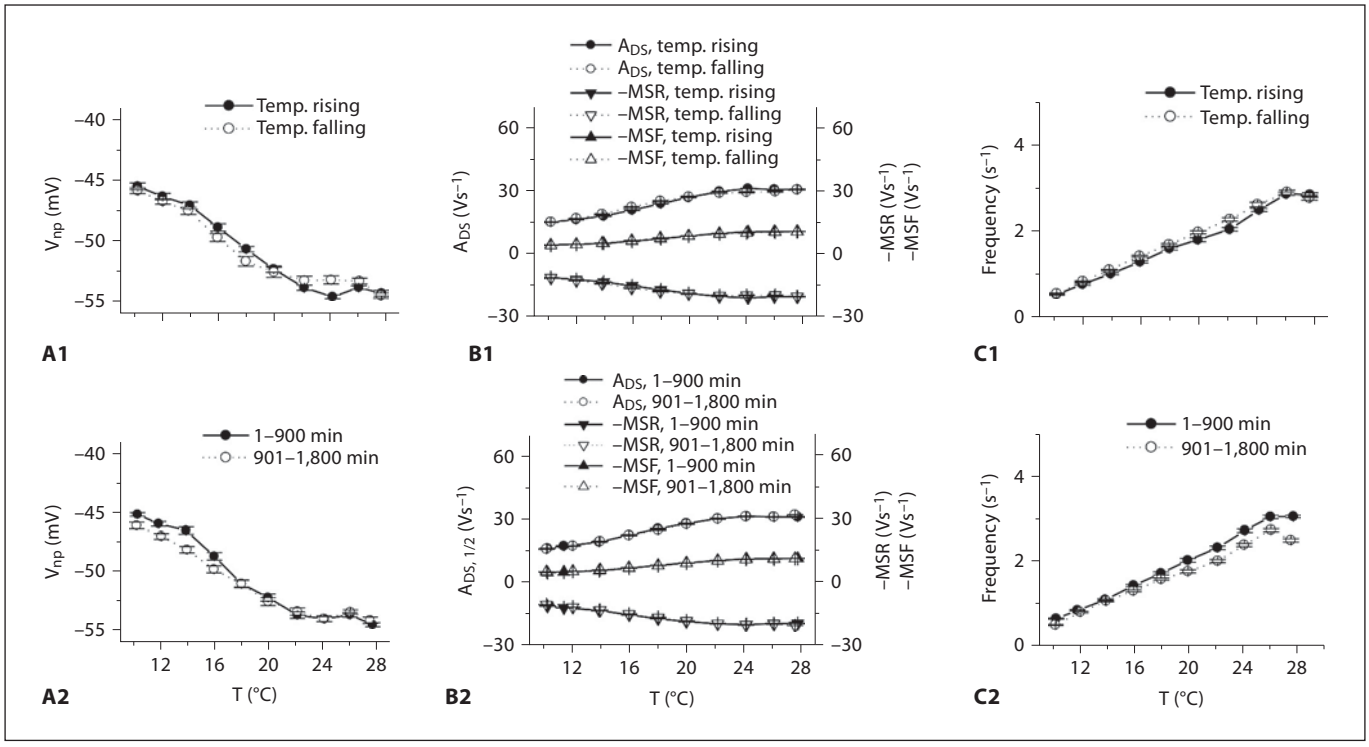

Fig. 6. Increases in AP parameters with temperature. Plots of V_{np}, A_{DS}, and Frequency (during the rising and falling phases of temperature change) are shown in **A1**, **B1**, and **C1**, respectively. Plots of –MSF and –MSR as a function of temperature are both shown in **B1**. V_{np}, A_{DS}, and Frequency (from 1 to 900 min and from 901 to 1,800 min) are shown in **A2**, **B2**, and **C2**, respectively. The parameters –MSF and –MSR as a function of temperature are both displayed in **B2**. Although the value of V_{np} decreased as the temperature increased, the absolute value of V_{np} ($|V_{np}|$) increased as the temperature increased.

of 14 AP parameters than used in former experiments. Moreover, we used *Aplysia* neural cells, which remain alive for a very long time in vitro; in experiment A, data were acquired continuously for over 60 h. Thus, it was possible to obtain data for 14 AP parameters that were dependent on a physical variable such as the temperature in *Aplysia* cells with relatively small error bars. We can be assured of the reproducibility with living experimental targets by examining the variation in the parameters recorded. Accordingly, we found that the 14 defined parameters were influenced by temperature in a highly reproducible manner.

Temperature-driven changes in AP parameters could affect the function of a neuron by changing the conduction velocity in the afferent axon as well as the firing rate [22]. Considering the importance of AP parameters in neuronal function [23], a question arises: how does the temperature affect these AP parameters in a neuron? Several studies have examined the temperature dependence of the intrinsic membrane conductance influenced by ion channel conductance. For example, Thompson et al. [24] found an increase in Ca^{2+}-activated K^+ conductance at a low temperature in hippocampal neurons in vitro. In addition, it was reported that alterations in temperature have a critical role in the conformational changes seen in a voltage-gated potassium channel, leading to their activation and inactivation [25]. Although they remain elusive in *Aplysia* neurons, transient receptor potential channels, which are nonselectively permeable to cations, are thought to be a group of ion channels used in animals to sense hot or cold sensations by being activated by a change of temperature [26]. Indeed, Chen et al. [27] reported that transient receptor potential-like channels contribute to the firing pattern of APs in the modified Hodgkin-Huxley neuron model. It is unclear how a temperature alteration can affect the specific ionic conductance that is responsible for the changes in the 14 AP parameters in our *Aplysia* model.

In order to address this issue, we aim to eventually develop nonlinear differential equations based on our recorded data for the 14 AP parameters and their temperature-dependent changes. Although the Hodgkin-Huxley-type Huber-Brown cold receptor model can simulate the temperature dependences of cold receptors [28, 29], a computer simulation model that explains the temperature dependence of the firing patterns in *Aplysia* neurons has not yet been found. The temperature-dependent reproducible properties of the 14 AP parameters described in this study can be considered as the basis for setting up a set of nonlinear differential equations that approximate the temperature-dependent firing patterns of neurons in *Aplysia*. However, because it is not easy to set up a system of equations using these results, it is necessary to perform another experiment to obtain the quantitative temperature-dependent properties of the APs. When the temperature was increased from 11 to 32°C, we found that seven firing patterns of the neurons in *Aplysia* changed sequentially from the silent state to beating, doublets, beating-chaos, bursting-chaos, square-wave bursting, and bursting-oscillation patterns [30]. In addition, as the temperature was decreased, the spiking patterns changed in reverse order. It would be beneficial to develop equations using scaling factors that depend on temperature and to trace whether alterations in temperature play a critical role in voltage-gated channels. Finally, it will be interesting to analyze the temperature-dependent properties of the 14 AP parameters using such equations.

Concluding Remarks

To determine functional relations that describe the temperature dependences of AP parameters, better experimental tools than those used in previous experiments were required. Using these more advanced tools, we performed experiments on long-lived in vitro *Aplysia* neural cells. In this paper, the AP parameters were analyzed and calculated using the data from an experiment with a cell from the abdominal ganglion of *A. juliana* to quantitatively understand the temperature dependences of the AP parameters. The basic experimental results relating to the temperature dependences of the 14 AP parameters displayed in figures 2 and 4–6 can be summarized as 3 findings:

(1) Nine AP parameters were found to decrease with increasing temperature: A_{AP}, V_{pp}, ISI, Δt_{r1}, Δt_{r2}, Δt_{f1}, Δt_{f2}, $\Delta t_{AP,\ 1/2}$, and $\Delta t_{DS,\ 1/2}$. Five AP parameters were found to increase with temperature: Frequency, $|\ V_{np}\ |$, A_{DS}, $|\ -MSR\ |$, and $|\ -MSF\ |$.

(2) Two AP parameters were characterized by larger values during the falling phases than during the rising phases of temperature change: Frequency and Δt_{f1}. Three AP parameters were characterized by larger values during the rising phases than during the falling phases of temperature change: ISI, $\Delta t_{r1,}$ and Δt_{f2}. However, if errors are considered, little difference is found between the rising and falling phases.

(3) Six AP parameters were characterized by larger values between 1 and 900 min than between 901 and 1,800 min: $A_{AP,}$ $V_{pp,}$ Frequency, $\Delta t_{AP,\ 1/2}$, $\Delta t_{r2,}$ and Δt_{f1}. Two AP parameters were characterized by larger values between 901 and 1,800 min than between 1 and 900 min: ISI and Δt_{r1}. However, if errors are considered, little difference is found between the first and last 15 h.

Acknowledgments

We thank Dr. Duck-Gun Park for the help provided during the experiments. K.-H.H. wrote the program in C++ to analyze our measured data, and we thank Prof. Kyung Ho Cho for improving the program for us. N.G.H. is most grateful to Prof. Jang-Ho Cha for his helpful advice and suggestions throughout the course of this work and for his generosity in allowing experiments to be conducted at the *Massachusetts General Hospital*. This work was supported by a research grant from Jeju National University in 2007. B.-K.K. was supported by the National Creative Research Initiative Program and the WCU program. K.L. was supported by the Basic Science Research Program of the Ministry of Education, Science and Technology (2011-0028240).

References

1 Murray RW: The effect of temperature on the membrane properties of neurons in the visceral ganglion of *Aplysia*. Comp Biochem Physiol 1966;18:291–303.

2 Hodgkin AL, Katz B: The effect of temperature on the electrical activity of the giant axon of the squid. J Physiol 1949;109:240–249.

3 Kerkut GA, Ridge RM: The effect of temperature changes on the activity of the neurons of the snail *Helix aspersa*. Comp Biochem Physiol 1962;5:283–295.

4 Dalton JC, Hendrix DE: Effects of temperature on membrane potentials of lobster giant axon. Am J Physiol 1962;202:491–494.

5 Stephens PJ, Frascella PA, Mindrebo N: Effects of ethanol and temperature on a crab motor axon action potential: a possible mechanism for peripheral spike generation. J Exp Biol 1983;103:289–301.

6 Heitler WJ, Edwards DH: Effect of temperature on a voltage-sensitive electrical synapse in crayfish. J Exp Biol 1998;201:503–513.

7 Burrows M: Effects of temperature on a central synapse between identified motor neurons in locust. J Comp Physiol A 1989;165:687–695.
8 Frankenhaeuser B, Moore LE: The effect of temperature on the sodium and potassium permeability changes in myelinated nerve fibres of *Xenopus laevis*. J Physiol 1963;169:431–437.
9 Vilim ES, Cropper EC, Price DA, Kupfermann I, Weiss KR: Release of peptide cotransmitters in *Aplysia*: regulation and functional implications. J Neurosci 1996;16:8105–8114.
10 Gardner D, Stevens CF: Rate-limiting step of inhibitory post-synaptic current decay in *Aplysia* buccal ganglia. J Physiol 1980;304:145–164.
11 Zhurov Y, Brezina V: Temperature compensation of neuromuscular modulation in *Aplysia*. J Neurophysiol 2005;94:3259–3277.
12 Redman RS, Berry RW: Temperature-dependent peptidergic feedback: potential role in seasonal egg laying in *Aplysia*. J Neurosci 1991;11:1780–1785.
13 Carpenter DO, Alving BO: A contribution of an electrogenic Na^+ pump to membrane potential in *Aplysia* neurons. J Gen Physiol 1968;52:1–21.
14 Carpenter DO: Temperature effects on pacemaker generation, membrane potential, and critical firing threshold in *Aplysia* neurons. J Gen Physiol 1967;50:1469–1484.
15 Marchiafava PL: The effect of temperature change on membrane potential and conductance in *Aplysia* giant nerve cell. Comp Biochem Physiol 1970;34:847–852.
16 Fletcher SD, Ram JL: High temperature induces reversible silence in *Aplysia* R15 pacemaker neuron. Comp Biochem Physiol 1991;98A:399–405.
17 Hakozaki SH, Matsumoto M, Sasaki K: Temperature-sensitive activation of G-protein regulating the resting membrane conductance of *Aplysia* neurons. Jpn J Physiol 1989;39:115–130.
18 Lim CS, Chung DS, Kaang B-K: Partial anatomical and physiological characterization and dissociated cell culture of the nervous system of the marine mollusc *Aplysia kurodai*. Mol Cells 1997;7:399–407.
19 Johnston D, Wu SM-S: Foundation of Cellular Neurophysiology. Cambridge, MIT Press, 1995.
20 Hille B: Ion Channels of Excitable Membranes, ed 3. Sunderland, Sinauer, 2001.
21 Moffett S, Wachtel H: Correlations between temperature effects on behavior in *Aplysia* and firing patterns of identified neurons. Mar Behav Physiol 1976;4:61–74.
22 French AS: The effects of temperature on action potential encoding in the cockroach tactile spine. J Comp Physiol A 1985;156:817–821.
23 Wang LY, Fedchyshyn MJ, Yang YM: Action potential evoked transmitter release in central synapses: insights from the developing calyx of Held. Mol Brain 2009;2:36.
24 Thompson SM, Masukawa LM, Prince DA: Temperature dependence of intrinsic membrane properties and synaptic potentials in hippocampal CA1 neurons in vitro. J Neurosci 1985;5:817–824.
25 Tiwari JK, Sikdar SK: Temperature-dependent conformational changes in a voltage-gated potassium channel. Eur Biophys J 1999;28:338–345.
26 Yang F, Cui Y, Wang K, Zheng J: Thermosensitive TRP channel pore turret is part of the temperature activation pathway. Proc Natl Acad Sci USA 2010;107:7083–7088.
27 Chen BS, Lo YC, Lius YC, Wu SN: Effects of transient receptor potential-like current on the firing pattern of action potentials in the Hodgkin-Huxley neuron during exposure to sinusoidal external voltage. Chin J Physiol 2010;53:423–429.
28 Braun HA, Huber MT, Dewald M, Schäfer K, Voigt K: Computer simulation of neural signal transduction: the role of nonlinear dynamics and noise. Int J Bifurcation Chaos Appl Sci Eng 1998;8:881–889.
29 Du Y, Lu Q, Wang R: Using interspike intervals to quantify noise effects on spike trains in temperature encoding neurons. Cogn Neurodyn 2010;4:199–206.
30 Hyun NG, Hyun K-H, Hyun K-B, Han J-H, Lee K, Kaang B-K: A computational model of the temperature-dependent changes in firing patterns in *Aplysia* neurons. Korean J Physiol Pharmacol 2011;15:371–382.